ФИЗИКА

UDC 537.533
IRSTI 55.22.19
https://doi.org/10.47526/2025-4/2524-0080.38

Dossymov Y[1]
[1]PhD, Khoja Akhmet Yassawi International kazakh-turkish university, (Kazakhstan, Turkestan), e-mail: dossymov.elmurat@ayu.edu.kz

INVESTIGATIONS OF THE SURFACE MORPHOLOGY OF Mn_4Si_7

Mn_4Si_7 БЕТТІК МОРФОЛОГИЯСЫН ЗЕРТТЕУ

ИССЛЕДОВАНИЯ МОРФОЛОГИИ ПОВЕРХНОСТИ Mn_4Si_7

Abstract. *In this work, we studied the surface morphology of a film of higher manganese silicide before and after heating. The mechanism of formation of a film of higher manganese silicide has been studied. The resulting silicon film was formed on the surface of SiO_2/Si or mica by magnetron sputtering. The morphology, composition, electrical and optical properties of bulk samples and Mn4Si7 vacuum coatings obtained by magnetron sputtering on the SiO2/Si structure have been studied. It is shown that manganese silicide coatings with a thickness of about 150 nm are similar in properties to bulk Mn4Si7 and have a homogeneous fine-grained semiconductor structure characterized by thermal sensitivity up to 20-30 Mv per degree. In addition, the article presents the electrophysical properties of films of high manganese silicide obtained by the authors by magnetron sputtering. Heated Mn4Si7-146 nm coated films have a homogeneous structure with fine grains, which is due to the sufficient coating density. Since Mn4Si7 nanoclusters are semiconductor materials, it can be assumed that energy barriers for charge carriers will exist at the interface of a nanocluster with an amorphous phase separating this phase. The increase in thermal sensitivity from 0 mv/K to 20 MV/K up to 800 K is explained by the disappearance of energy barriers for charge carriers at the nanocluster-amorphous phase interface due to the ordering of nanoclusters. The change from 20 mv/K to 28 MV/K during cooling is explained by the appearance of structural relaxation in the amorphous phase.*

Key words: *morphology, thermal, Mn, Si, spectrometr.*

Аңдатпа. *Бұл жұмыста біз қыздыруға дейін және одан кейін жоғары марганец силикидінің қабықшасының беттік морфологиясын зерттедік. Жоғары марганец силикидінің қабықшасының түзілу механизмі зерттелді. Алынған кремний пленкасы Магнетрондардың шашырауы Нәтижесінде SiO2/Si немесе слюда бетінде пайда болды. Сусымалы үлгілердің морфологиясы, құрамы, электрлік және оптикалық қасиеттері Және SiO2/Si құрылымында магнетрондардың шашырауы нәтижесінде Алынған mn4si7 вакуумдық жабындары зерттелді. Қалыңдығы шамамен 150 нм болатын марганец силикидті жабындарының қасиеттері бойынша сусымалы Mn4Si7-ге ұқсас және бір градусқа 20-30 Мв-қа дейінгі жылу сезімталдығымен сипатталатын біртекті ұсақ түйіршікті жартылай өткізгіш құрылымы бар екендігі көрсетілген.. Сонымен қатар, мақалада авторлар магнетронды шашырату арқылы алған жоғары марганецті силикидті қабықшалардың электрофизикалық қасиеттері келтірілген. Қыздырылған Mn4Si7-146 нм қапталған қабықшалар жұқа түйіршіктері бар біртекті құрылымға ие, бұл жабынның жеткілікті тығыздығына байланысты. Mn4si7 нанокластерлері жартылай өткізгіш материалдар болғандықтан, заряд тасымалдаушылар үшін энергетикалық кедергілер осы фазаны бөлетін аморфты фазасы бар нанокластердің интерфейсінде болады деп болжауға болады. Жылу сезімталдығының 0 мв/К-ден 20 МВ/К-ге дейін 800 К-ге дейін жоғарылауы нанокластерлердің реттелуіне байланысты нанокластер-аморфты фазалық интерфейсте заряд тасымалдаушылар үшін энергетикалық кедергілердің жойылуымен түсіндіріледі. Салқындату кезінде 20 мв/К-ден 28 МВ/К-ге дейінгі өзгеріс аморфты фазада құрылымдық релаксацияның пайда болуымен түсіндіріледі.*

Негізгі сөздер: *морфология, жылу, Mn, Si, спектрометр.*

Аннотация. *В данной работе мы изучили морфологию поверхности пленки силицида марганца с высоким содержанием марганца до и после нагревания. Изучен механизм образования пленки силицида марганца с высоким содержанием марганца. Полученную пленку кремния формировали на поверхности SiO2/Si или слюды методом магнетронного распыления. Изучены морфология, состав, электрические и оптические свойства объемных образцов и вакуумных покрытий Mn4Si7, полученных методом магнетронного распыления на структуру SiO2/Si. Показано, что покрытия из силицида марганца толщиной около 150 нм по свойствам аналогичны объемным Mn4Si7 и имеют однородную мелкозернистую полупроводниковую структуру, характеризующуюся термочувствительностью до 20-30 Мв на градус. Кроме того, в статье представлены электрофизические свойства пленок силицида марганца с высоким содержанием марганца, полученных*

авторами методом магнетронного распыления. Пленки с покрытием Mn4Si7 толщиной 146 нм имеют однородную структуру с мелкими зернами, что обусловлено достаточной плотностью покрытия. Поскольку нанокластеры Mn4Si7 являются полупроводниковыми материалами, можно предположить, что энергетические барьеры для носителей заряда будут существовать на границе раздела нанокластера с аморфной фазой, разделяющей эту фазу. Увеличение тепловой чувствительности с 0 мВ/К до 20 МВ/К и вплоть до 800 К объясняется исчезновением энергетических барьеров для носителей заряда на границе раздела нанокластер-аморфная фаза за счет упорядочения нанокластеров. Изменение с 20 мВ/К до 28 МВ/К при охлаждении объясняется появлением структурной релаксации в аморфной фазе.

***Ключевые слова**: морфология, термический анализ, Mn, Si, спектрометр.*

Introduction

The purpose of this work is to study changes in the electronic structure of the silicon surface during the implantation of Va ions and subsequent thermal annealing. The surface electronic properties of semiconductors, in particular Si, are in the focus of many researchers. It should be noted that proper surface states are inherent in the free surface of the crystal, in contrast to improper surface states due to the presence of foreign atoms on the surface or marginal surface states caused by the presence of a defective structure in the near-surface region of the crystal. Defects occur in ion-implanted silicon layers at low doses of ion implantation. In this case, the appearance of donor or acceptor impurity levels in the silicon band gap should be expected. Ion implantation leads to a violation of the crystal structure of the initial silicon up to amorphization. Of the variety of processes occurring during the implantation of ions into silicon, our main attention was paid to the study of the effect of implantation of high-dose ions on the electron-band structure of silicon. Silicon single crystals Si(111) and Si(100), a type with a resistivity of p=3000 ohms×cm, were chosen as the substrate. The purification of the initial crystal was carried out by thermal heating in an ultrahigh vacuum p = 10-7 Pa in two stages: for a long time (for 60-120 minutes) at a temperature of T = 1000 K and for a short time (for 30-60 seconds) at T = 1550 K.

Slow electron diffraction (DME), electron auger spectrometry (EOS), spectroscopy of characteristic electron energy losses ((SHAPE), photoelectron spectroscopy (FES), raster electron high-resolution microscopy (SEM), X-ray energy dispersive spectroscopy.

Materials and Methods

Silicon single crystals Si(111) and Si(100), a type with a resistivity of p=3000 ohms×cm, were selected as the substrate. Purification of the initial crystal was carried out by thermal heating in an ultrahigh vacuum p = 10-7 Pa in two stages: for a long time (for 60-120 minutes) at a temperature of T = 1000 K and for a short time (for 30-60 seconds) at T = 1550 K.

Slow electron diffraction (DME), electron auger spectrometry (EOS), spectroscopy of characteristic electron energy losses (SHPE), photoelectron spectroscopy (FES), raster electronic high-resolution microscopy (SEM), X-ray energy dispersive spectroscopy.

Scanning electron microscopy allows obtaining general and local information about the microstructure of a sample with high accuracy. The resolution of a scanning electron microscope depends on the diameter of the electron beam and on the size of the interaction area of the electron probe with the sample. Thus, depending on the average atomic number of a substance, by changing the accelerating voltage from 30 to 1 kV, it is possible to obtain data on the microstructure of a sample from a depth of several microns to hundreds of nanometers. To achieve the best resolution, a high signal-to-noise ratio is required with the smallest possible size of the scanning probe. The minimum beam size for a thermocathode is ~5 microns, while for a cathode with field emission ~5-25 nm [5]. The best resolution in scanning electron microscopy to date has been obtained using an electron gun with field emission and reaches several angstroms. Image registration takes place either in secondary or in backscattered electrons. The contrast in electron microscopic images obtained in secondary electrons (energy less than 50 eV) depends most strongly on the surface relief. Whereas the contrast in the SEM images obtained in the registration mode of backscattered

electrons with an energy from 50 eV up to the energy of the primary beam is mainly associated with a change in the average atomic number of the substance over the sample area. Thus, a compositional or "2-contrast" is formed. Using various modes of recording SEM images, it is possible to obtain information about the morphology of the sample and identify the release of other phases.

Modern scanning electron microscopes make it possible to analyze the chemical composition of a sample by registering the characteristic X-ray radiation that occurs when an electron beam interacts with a sample (the method of energy dispersive spectroscopy (EMF)). The method allows for qualitative and quantitative analysis of the chemical composition and determination of the concentration practically any elements from beryllium to california in the concentration range from tenths of a percentage by weight to 100%. For massive crystals, the resolution is limited to 1 micron, while in thin sections, the resolution of the method reaches units of a nanometer.

Currently, the use of scanning electron microscopy together with energy dispersive spectroscopy is an integral part of every complex structural study.

An example of the successful application of scanning electron microscopy to the study of the structure of SCM is the work of Luo and co-authors [1], in which polycrystalline samples of SCM were synthesized by arc plasma melting. An important structural feature of the samples of higher manganese silicides is the formation of secretions of the cubic phase of manganese monosilicide MnSi. In [3], the structure of the samples was first investigated by powder X-ray diffractometry, which did not reveal the presence of MnSi in the HCM crystal. However, using the SEM method in the mode of backscattered electrons, micron-scale MnSi phase separations were detected. The absence of reflexes on radiographs from the manganese monosilicide phase was explained by its low concentration.

The morphology of the samples was analyzed using a scanning electron bi-beam microscope Scios FEI. The images were taken from all six samples at different magnifications and using different sensors. First, to have a general idea of the morphology, consider the surface of the samples at a small magnification. The first series of images was obtained with a magnification of 15 thousand times. For the convenience of comparing samples with annealing and without annealing, the images will be in pairs (A-A1, B-B1, C-C1). Figures 1 and 2 show SEM images of the surface of the film A. It can be seen that after annealing (Fig.2), the sample acquired a noticeably denser structure, the pores disappeared, and the surface became much more homogeneous. Apparently, this is due to the crystallization of the film as a result of annealing. When analyzing the morphology of the film surface, it is clearly visible that the sample turned out to be less successful – it is covered with bubbles (Fig.3). And even though the bubbles shrank noticeably after exposure to temperature (Fig.4), unfortunately, this did not correct the overall picture. The origin of bubbles will be analyzed in more detail in the next experiment [1-5].

Results

Currently, much attention is being paid to the problem of saving energy resources, therefore, interest in materials with thermoelectric properties is growing again. Among such materials, the highest manganese silicide Mi811.75 (HSM) is among the most promising, since its thermoelectric efficiency reaches 0.4 in the temperature range of 20-800 °C. One of the significant advantages of higher manganese silicide is the environmental friendliness of the initial components and the low cost of production. HCM films and crystals are important for practical applications in micro- and nanoelectronics, optoelectronics, microsensory, as well as for the creation of thermogenerators, thermal batteries and other thermoelements based on them. The transition from bulk BCM crystals to thin films makes it possible to obtain thermoelements with different physical properties due to the influence of dimensional factors, the appearance of quantum effects, and the possibility of creating nanoheterostructures. The creation of new devices based on films of higher manganese silicide with specified properties requires a detailed study of their micro- and nanostructure, phase

and chemical composition, as well as solid-phase reactions occurring in the Mp-81 system at elevated temperatures [6].

To obtain the most complete and statistically reliable information about the structure of HSM films, as well as about the phase and chemical composition at the macro and nanoscale, it is possible to use a complex of modern methods of analytical electron microscopy. Thus, scanning electron microscopy together with energy dispersive spectrometry allows us to obtain integral information about the microstructure and chemical composition of the material; diffraction of backscattered electrons is necessary to determine the phase composition, blockiness, orientation analysis; transmission electron microscopy (TEM) and high-resolution electron microscopy (HREM) are used for local analysis of the phase and chemical composition of the matrix crystal and secretions and to study the structure of the interface between the secretions and the matrix crystal [7].

For samples C and C1, the difference in the morphology of the film surface before and after annealing is very large (Fig. 5, Fig.6). The surface of the unburned sample is even more uniform than that of the corresponding sample A. This is obviously due to the fact that the citall is more homogeneous than mica [8]. The damage on the surface is of mechanical rather than chemical origin. After thermal annealing, an inhomogeneous "island" structure appears on the surface. Moreover, massive clusters form in some places on the surface (Fig.6). For a more detailed study of changes in the morphology of the surface of selected films as a result of thermal annealing, let's consider SEM images obtained with an increase of 60 thousand times [9].

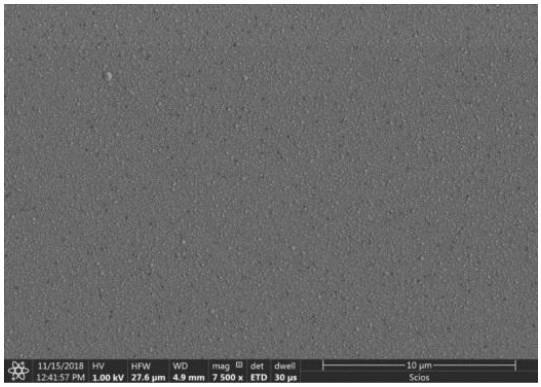

Fig. 1. SEM image of the sample surface A

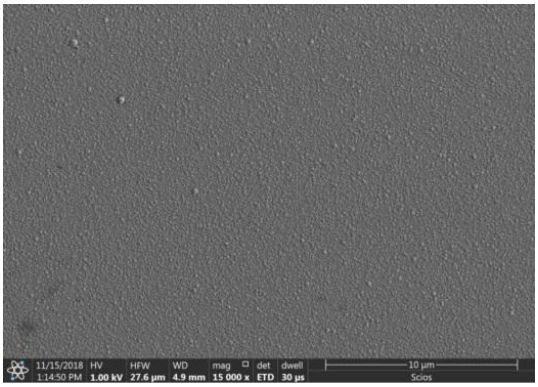

Fig. 2. REM image.

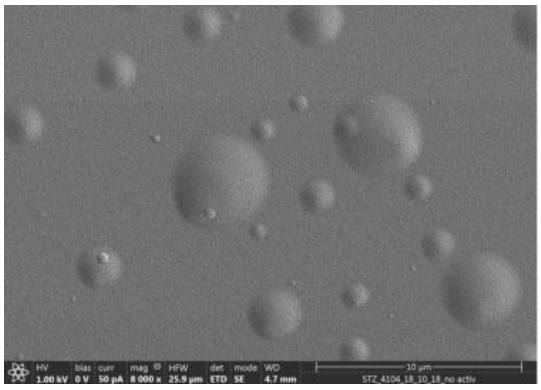

Fig. 3. SEM image of the surface of the sample B.

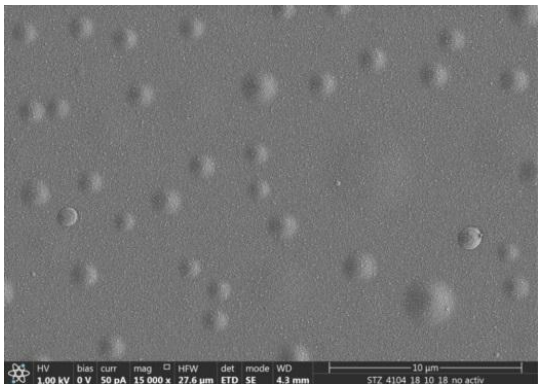

Fig. 4. SEM image of the sample surface in 1.

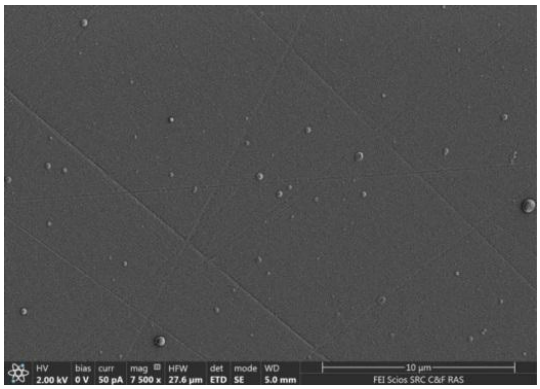

Fig. 5. SEM image of the surface of sample B1.

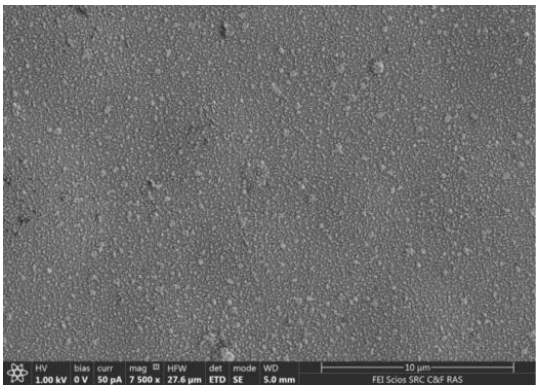

Fig. 6. SEM image of the sample surface from 1.

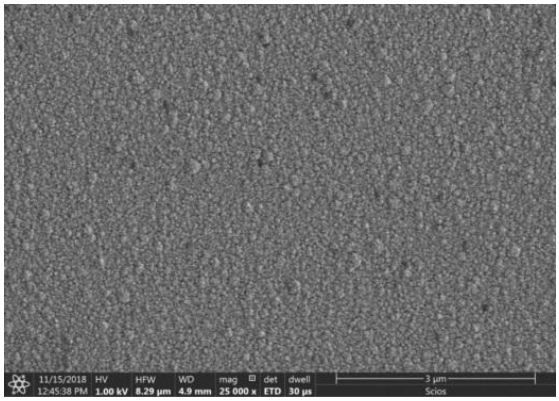

Fig.7. SEM image of the surface of sample A.

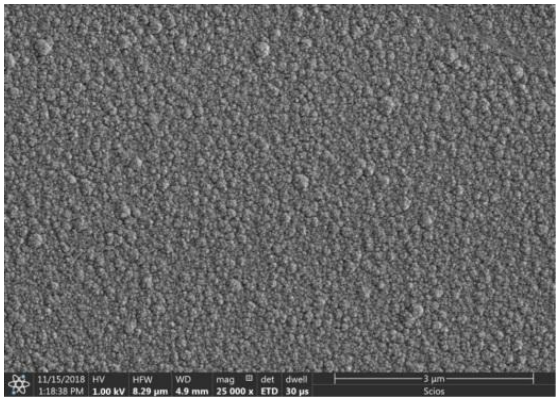

Fig.8. SEM image of the surface of sample A1

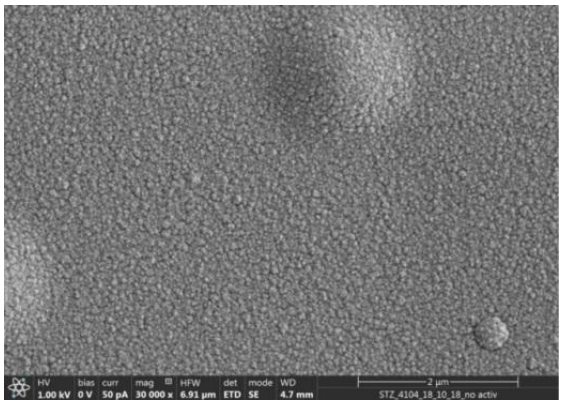

Fig.9. SEM image of the sample surface B.

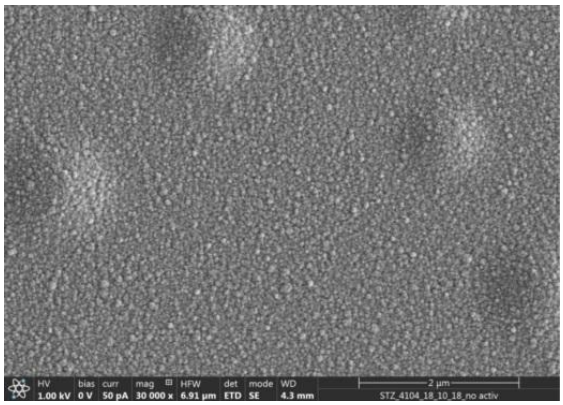

Fig.10. SEM image of the surface of the sample B1.

Figures 7 and 8 show SEM images of the surface of sample A and A1 without annealing and after annealing, obtained with an increase of 60,000 times. It can be seen that the surface without heat treatment (Fig.7) is smooth, and after heat treatment it becomes dense, homogeneous with a granular structure (Fig.8).

From a comparison of the SEM images of samples B and B1 shown in Fig.9 and Fig.10, it can be seen that the bubbles after annealing have a smaller diameter and they protrude less above the surface. Thermal annealing of the sample leads to a compaction of the film structure and to a significant narrowing of the pores.

Figures 11 and 12 show SEM images of the surface of the sample C and C1 without annealing and after annealing, obtained with an increase of 60,000 times. It can be seen that the surface of the film before annealing is the densest, if you do not take into account the presence of small clumps of matter and furrows. Film C is the most promising in comparison with other films. After annealing, the film structure changed significantly, Fig.12. Apparently, the film, and possibly the substrate, began to bubble and boil in places when heated, then the bubbles burst, forming craters at the bottom of which the substrate is visible. Figures 12, 13, and 14 show SEM images of the film surface, crater boundary, and substrate surface, respectively.

Conclusion

In this work, a comprehensive investigation of the morphology, structure, and electrophysical properties of thin films of high-manganese silicide Mn_4Si_7 deposited by magnetron sputtering on SiO_2/Si and mica substrates before and after thermal annealing was carried out. The obtained results allow a number of fundamentally important conclusions to be drawn, which are significant both from fundamental and applied perspectives.

It was established that the initial state of Mn_4Si_7 films is characterized by a strong dependence of surface morphology on the substrate type and deposition conditions. In the as-deposited samples, pores, bubbles, and local inhomogeneities are observed, which are associated with incomplete crystallization, residual mechanical stresses, and trapped gaseous inclusions. These effects are particularly pronounced in films deposited on less homogeneous substrates, where the formation of a defective structure is caused by differences in thermal expansion coefficients and weak adhesion at the film–substrate interface.

Thermal annealing leads to a qualitative modification of the film surface morphology. It is shown that heating results in structural densification, elimination of pores, and the formation of a homogeneous fine-grained morphology, indicating the occurrence of recrystallization and structural relaxation processes. The increase in the degree of crystallinity is accompanied by a reduction in the fraction of the amorphous phase and a more uniform grain size distribution, which is crucial for stabilizing the electronic and thermal properties of the material.

Special attention should be paid to the revealed role of the nanocluster structure of Mn_4Si_7. The films represent a system of semiconducting nanoclusters separated by thin interlayers of an amorphous phase. In the initial state, energy barriers for charge carriers are formed at the “nanocluster–amorphous matrix” interfaces, leading to low thermoelectric voltage and suppressed electrical conductivity. During heating, ordering of the nanoclusters and a reduction in the height of the potential barriers occur, which explains the sharp increase in thermal sensitivity up to 20–30 mV/K at temperatures up to 800 K.

The change in thermoelectric characteristics during cooling is irreversible in nature and is associated with structural relaxation effects in the amorphous phase. The emergence of internal stresses and local atomic rearrangements leads to a further increase in thermal sensitivity up to 28 mV/K, indicating a complex interplay between microstructure, phase state, and charge transport in Mn_4Si_7 films.

A comparative analysis of different samples showed that the best properties are exhibited by films with the highest density and the minimum number of morphological defects prior to annealing. This allows the conclusion that not only thermal treatment but also the initial deposition parameters play a key role in the formation of the functional characteristics of the material.

Overall, the results confirm that Mn_4Si_7 thin films with a thickness of approximately 150 nm are close to bulk samples in terms of their structural and electrophysical properties, while possessing additional advantages associated with size effects and the possibility of nanostructure control. The obtained data deepen the understanding of morphology formation and charge transport mechanisms in high-manganese silicides and provide a scientific basis for the targeted design of thermoelectric elements, microsensors, and micro- and nanoelectronic devices based on Mn_4Si_7.

References

1. Kuznetsova, V. S., Novikov, S. V., Nichenametla, C. K., Calvo, J., & Wagner-Reetz, M. (2019). *Semiconductors*, *53*(6), 775–779. https://doi.org/10.1134/S1063782619060101
2. Ranganathan, S., & Heimendahl, M. (1981). *Journal of Materials Science, 16*, 2401–2404.
3. Grabchikov, S. S. (2006). *Amorfnyy elektroliticheski osazhdennye metallicheskie splavy* [Amorphous electrolytically deposited metal alloys]. Izd. Tsentr BGU.
4. Hicks, L., & Dresselhaus, M. (1993). *Physical Review B, 47*, 12727–12731.
5. Hochbaum, A. I., Chen, R., Delgado, R., et al. (2008). *Nature, 451*(7175), 163–167. https://doi.org/10.1038/nature06381
6. Kanatzidis, M. G. (2010). *Chemistry of Materials, 22*(3), 648–659. https://doi.org/10.1021/cm902195j
7. Iqbal, Z., Webb, A., & Veprek, S. (1980). *Applied Physics Letters, 36*(2), 163–165.
8. Petermann, J. (1991). *Bulletin of the Institute for Chemical Research (Kyoto University), 69*(2), 84–91.
9. Brahma, R., & Ghanashyam, K. (2012). *Bulletin of Materials Science, 35*(4), 551–560.
10. Kuksenova, L. I., Gerasimov, S. A., Alekseeva, M. S., & Gromov, V. I. (2018). Vliyaniye vakuumnoy khimiko-termicheskoy obrabotki na iznosostoykost' staley VKS-7 i VKS-10 [Effect of vacuum chemical-thermal treatment on the wear resistance of VKS-7 and VKS-10 steels]. *Aviatsionnye materialy i tekhnologii*, (1), 3–8. https://doi.org/10.18577/2071-9140-2018-0-1-3-8
11. Gromov, V. I., et al. (2016). Vliyaniye ostatochnogo austenita na strukturu i svoystva diffuzionnogo sloya stali martensitnogo klassa posle vakuumnoy tsementatsii [Effect of retained austenite on the structure and properties of the diffusion layer of martensitic-class steel after vacuum carburizing]. *Aviatsionnye materialy i tekhnologii*, (4), 3–8. https://doi.org/10.18577/2071-9140-2016-0-4-3-8
12. Edenhofer, B. (1999). An overview of advances in atmosphere and vacuum heat treatment. *Heat Treatment of Metals, 26*(1), 1–5.

Авторлар туралы мәліметтер

№	Аты-жөні, ғылыми дәрежесі, жұмыс немесе оқу орны, қала, ел, автордың e-mail мекенжайы, ұялы телефон нөмірі
1	**Досымов Е.** – PhD, Қожа Ахмет Ясауи атындағы Халықаралық қазақ-түрік университеті, Түркістан қ., Қазақстан, e-mail: dossymov.elmurat@ayu.edu.kz
	Dossymov Y – PhD, Khoja Akhmet Yassawi International Kazakh-Turkish University, Turkistan, Kazakhstan,e-mail: dossymov.elmurat@ayu.edu.kz
	Досымов Е. – PhD, Международный казахско-турецкий университет имени Ходжи Ахмеда Ясави, г. Туркестан, Казахстан, e-mail: dossymov.elmurat@ayu.edu.kz